Progress in Physics of Applied Materials 6 (2026), Serial Number 11, 99-110

Semnan University

Progress in Physics of Applied Materials

journal homepage: https://ppam.semnan.ac.ir/

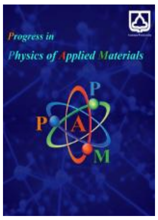

Correlation Between Fermi-Energy, Chemical Shifts, and Surface Plasmon Resonance in Cu and Zn Compounds under X-ray Illumination

Tika Ram[a], Ajay Kumar[b]*, Dinesh Kumar[c], Poonam Juneja[d], Sanjeev Rathore[e], Hari Krishan[f], Narinder Kumar[a]

[a] *Department of Physics, Uttaranchal Institute of Technology, Uttaranchal University, Dehradun-248007, Uttarakhand, India*

[b] *Department of Chemistry, School of Applied and Life Sciences, Uttaranchal Institute of Technology, Uttaranchal University, Dehradun-248007, Uttarakhand, India*

[c] *Uttar Pradesh State of Higher Education Council, Lucknow, Uttar Pradesh, India*

[d] *Department of Physics, Maitreyi College, University of Delhi, Delhi, India*

[e] *Department of Physics, Government Degree College, Badaun, -243601, Uttar Pradesh, India*

[f] *Department of Chemistry, Michigan Diagnostic LLC, 2611 Parmenter Blvd, Royal Oak, MI, USA 48073*

ARTICLE INFO

Article history:
Received: 16 September 2025
Revised: 31 October 2025
Accepted: 4 November 2025
Published online: 1 December 2025

Keywords:
Chemical shift;
Fermi energy;
Surface plasmon resonance;
Plasmon energy;
X-ray illumination.

ABSTRACT

This study represents an integrated theoretical framework that correlates copper (Cu) and zinc (Zn) compounds with variation in Fermi energy, chemical shifts, and surface plasmon resonance (SPR) under X-ray illumination. A simplified but conscientious model was developed to determine chemical shifts in X-ray K-absorption spectra based on Fermi energy differences between metals and their compound states. The model incorporates electron concentration, plasmon energy, and effective charge to predict more clearly the sign as well as the amount of chemical shift without depending on empirical adaptation. Experimental X-ray absorption data closely match the expected chemical shifts (2.7-6.0 eV for Cu compounds and 2.4-4.7 eV for Zn compounds), confirming the model's reliability. A correlation between Fermi energy and effective charge confirms that electron redistribution of compounds governs spectral edge shifts under X-ray illumination. Furthermore, the conceptual link between Fermi-level modulation and SPR behavior illustrates that variations in conduction electron density are influenced by X-ray illumination. This correlation reveals a consistent theoretical explanation for photo-induced plasmonic phenomena in Cu, Zn, and their compounds based materials. Overall, the suggested model enhances perception of the Fermi energy dependence of chemical shifts and extends its applicability to plasmonic materials. The current study offers a frontier analysis tool that will be used for the electronic and optical properties of transition-metal compounds.

1. Introduction

1.1. *Empirically*

Over the last three to five decades, extensive efforts have been made to provide several possible justifications for the reported magnitudes of chemical shifts during X-ray illumination. Efforts have been made to relate chemical shifts analytically through the covalent nature of the chemical bonding, valence state, and electronegativity state [1-4]. Salem et al. [5] tried to describe that the active charge (ionic) is responsible for such a shift of the edge during K-

---

* Corresponding author.
E-mail address: **ajay.tiwari1591@gmail.com**

Cite this article as:

Ram, T., Kumar, A., Kumar, D., Juneja, P., Rathore, S., Krishan, H. and Kumar, N., 2026. Correlation Between Fermi-Energy, Chemical Shifts, and Surface Plasmon Resonance in Cu and Zn Compounds under X-ray Illumination. *Progress in Physics of Applied Materials*, 6(2), pp.99-110. DOI: **10.22075/ppam.2025.39045.1170**

absorption in the case of vanadium for a few of its compounds. Joseph et al. [6] have given the explanation in the case of shifting of the K-edge during absorption for copper (Cu) by X-ray, while Joseph and Patra [7] measured such shifts in zinc (Zn) compounds by using the Synchrotron radiation source. Recently, Rudolph and Jacob [8] studied a clear correlation between Cu K-edge X-ray absorption spectroscopy (XAS) spectral features; their findings offer a reliable theoretical framework for interpreting *in situ* XAS spectra of Cu-based catalytic intermediates. The detection of a chemical shift during the assembly of adjacent absorption features in the fluorescence field of the K-edge X-ray confirms the occurrence of K-edge formation in Cu and Zn compounds (Fig. 1).

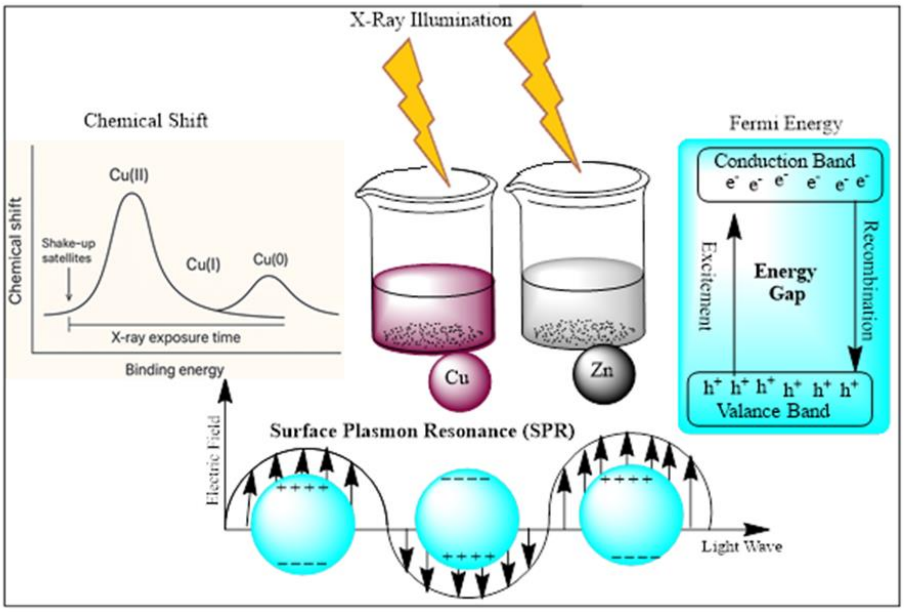

Fig. 1. Cu and Zn compounds Fermi energy, chemical shift, and surface plasmon resonance changes under X-ray illumination.

However, nobody stated that they were competent to provide objectively both magnitudes as well as indications of positive and negative (sign) noted chemical shifts. Investigations in many research projects show that the complexity of linking the experimentally proven changes in the edge of X-ray spectra and the measured value of the shifting of resonant frequency requires further methodological analysis. Some researchers believe that the variation concerning the chemical nature of an element (metal) that makes a composition is owing to the movement of the charge of electrons along a certain space [9, 10]. The Fermi level should alter during the shifting of these absorption edges [11-14].

1.2. Basic Theory

In the X-ray absorption spectra, the relevant edge relates to a switch of an underlying electron to the initial empty level (conducting level last portion E_C) beyond the Fermi energy level. During chemical combination, when a metal forms a compound, the energy of the X-ray absorption edge gets shifted. The energy difference between the absorption edge of a metal conduction band (E_C^M) and its semiconductor conduction band (E_C^S) is termed the chemical shift (ΔE_C). E_C^S and E_C^M are the sharp energy points (edge) of absorption of the relevant semimetal compound and metal, respectively.

During the observation of the curve of absorption by X-rays, the K-edge links to an initial inflection point. Likewise, in theory, one can also identify the initial inflection point in the observed curve due to X-ray emission, which corresponds to a transition from the highest valence band (E_{VS}) to the respective K-energy level. The metal shows variable spots, and its curves are formed due to absorption overlap. In this event, they together relate to the energy of the Fermi band (E_M^F), although during the situation of a compound (semimetal), the spots of inflection of emission and absorption never overlap, the E_{VS} are detached from the base of the conducting energy (E_{CS}) band through a break (or gap) by energy (E_g). Accordingly, a shift of resonant frequency is the variation in the absorption curves of a semimetal or semiconductor (S) and a metal (M). As a result, the chemical changes are described as:

$$(\Delta E_C) = E_C^S - E_C^M \tag{1}$$

However, in the case of metals, it is fairly well known that:

$$E_C^M = E_F^M \tag{2}$$

For intrinsic (undoped), non-degenerate semimetals, the bandgap is defined as,

$$E_g = E_{cs} - E_{vs} \tag{3}$$

The Fermi level of an undoped semimetal lies near mid-gap. Here, Equation 3 gives the minimum conduction-based subtraction by the valence band maximum. Energy band gap (Eg), between the conduction and valence bands, denotes the fundamental electronic transition energy governing the optical and electrical properties of the material. While for the Zn and Cu compounds/semi/partial metals, the energy of the Fermi level may be specified by [15]: $E_{FS} = \frac{1}{2}(E_{cs} + E_{vs}) + k_BT/2 \ln(N_{vs}/N_{cs})$ In semimetals, the Fermi level (E_{FS}) does not coincide with the conduction band edge (E_{CS}) due to the presence of an energy band gap (Eg) between the valence and conduction bands. The Fermi level lies within the band gap, and its position depends on the carrier concentration and doping type.

Where Ncs and Nvs are the effective densities of states and m_e^*, m_h^* the effective masses. For an intrinsic semimetal, the Fermi level can be expressed as:

$$E_{FS} = ½ (E_{cs} + E_{vs}) + k_BT/2 \ln (m_h^*/m_e^*) \quad (4)$$

Where E_{VS} is the valence band maximum, k is the Boltzmann constant, T is the temperature, and m_h^* and m_e^* are the effective masses of holes and electrons, respectively. In the case of n-type and p-type semimetals, the Fermi level shifts closer to the conduction or valence band edge, depending on the acceptor or donor concentration of the compounds. In the present model, this corrected treatment has been incorporated by considering the relative shift of Fermi levels between metallic and compound states rather than assuming direct equality. The correlation between the Fermi level position, electron concentration, and plasmon energy remains valid, but it now properly accounts for the physical constraints of semimetals such as ZnO and CuO, where the Fermi level resides within the band gap and moves according to charge redistribution during compound formation.

For simplicity, we use the mid-gap approximation. Considering Eqs. (3) and (4), we get $E_{FS} \approx E_{CS} - E_g/2$ For intrinsic semimetals such as ZnO and CuO, the Fermi level lies near the mid-gap, and the above relation should be applied. The approximation $E_{FS} \approx E_{CS}$ is valid only for metallic or highly doped systems where Eg is zero. This should be applied only when the material is intrinsic (or weakly doped) and when the correction term $k_BT/2 \ln (Nvs/Ncs)$ is small. For doped or degenerate semimetals (and for materials with large Eg), the above full expression should be used. The simplification $E_{FS} \approx E_{CS}$ is not valid for materials with a finite bandgap. It applies only to metallic systems or cases where Eg/2 is negligible compared to thermal energy. For intrinsic semimetals such as ZnO or CuO, Eg/2 must be retained to represent the Fermi level position accurately.

The parameter *Z*, representing the number of electrons contributing to collective plasma oscillations, has been chosen based on well-established free-electron and plasmonic models developed by Pines [16].

2. Experimental

2.1. Material Information

The study focuses on Cu and Zn metals, having well-known electronic structures and their commonly studied compounds due to their broad catalysis, sensing, and materials science. High-purity Cu and Zn were considered as reference metals, and their compounds have bonding nature, oxidation states, and ligand interactions that influence the X-ray absorption edges and associated chemical shifts [17]. In Zn, the compounds analyzed include zinc oxide (ZnO), zinc carbonate ($ZnCO_3$), zinc phosphate ($Zn_3(PO_4)_2$), and zinc nitrate ($Zn(NO_3)_2$). These materials cover a range of oxygenated, nitrogen-containing, and carbonate environments that allow investigation of electronic redistribution across diverse bonding situations. In copper, selected compounds include copper iodide (CuI), copper oxide (CuO), copper carbonate ($CuCO_3$), copper sulfate ($CuSO_4$), and copper acetate ($Cu(CH_3COO)_2$). These compounds represent halide, oxide, sulfate, organic, and carbonate environments, respectively, providing a comprehensive framework for studying both monovalent and divalent oxidation states of Cu. All compounds were considered in their standard crystalline forms, with molecular weights, densities, and valence electron counts obtained from standard chemical databases and literature values. These parameters were used as input for calculating the Fermi energy, plasmon energy, and ultimately the chemical shifts [18]. The careful selection of materials ensured that both experimental data from previous studies and theoretical calculations could be compared systematically, thereby validating the predictive framework developed in this work.

2.2. Method Information

The methodology applied in this study integrates theoretical modeling with reported experimental data to evaluate chemical shifts in the elements of Cu and Zn compounds. The central approach relies on correlating Fermi energy with plasmon oscillations, enabling the prediction of X-ray absorption edge shifts without direct reliance on synchrotron measurements. First, relevant physical constants and structural parameters such as molecular density (ρ), weight (M), and the number of conduction electrons contributing to plasma oscillations (Z) were obtained from literature values and standard chemical data sources.

These values were then used to calculate the plasmon energy ($\hbar\omega_p$) of each Cu- and Zn-based compound according to the standard density-dependent expression that relates $\hbar\omega_p$ to the conduction-electron density (ρ). For reference metals, experimental plasmon loss values were compared with theoretical calculations to validate the accuracy of the selected Z values. Next, the Fermi energy (E_F) was derived using Pines' relation (equation (5)), which relates EF to the plasmon energy. This calculation was performed for both metals (Cu and Zn) and their respective compounds. The chemical shift (ΔE_C) was then determined as the difference in Fermi energy between a pure metal and its corresponding compound, following equation (7). To evaluate the reliability of the model, the calculated chemical shifts were compared against experimentally observed values reported in earlier X-ray absorption studies [6,7,19-21]. Graphs were plotted to illustrate the different compounds, and additional comparisons were made with effective charge data obtained from previous studies [22, 23]. This method, while theoretical in formulation, was designed to reduce reliance on complex synchrotron experiments and instead provide a predictive framework for estimating chemical shifts across a wide range of Cu and Zn compounds. The combined use of plasmon energy, Fermi energy, and electron redistribution allows a more comprehensive understanding of the interplay between electronic structure and observed absorption edge shifts [24-26]. The incorporation of the more comprehensive work on the theoretically unexplained chemical shift of Cu and Zn compounds, as experimentally observed by some workers [23-25], leads to featuring more parameters like the electronic concentration and the temperature of the specimen, which may affect the collective excitations in Cu and Zn.

To learn the energy of the Fermi level of a semimetal, one can utilize the expression for the energy of the Fermi level plus the energy of the plasmon developed by Pines [16], like:

$$E_F = 3.68/r_s^2 \text{ ryd} = A(\hbar\omega_p)^{4/3} \text{eV} = 0.2948\ (\hbar\omega_p)^{4/3} \text{ eV} \qquad (5)$$

where A is a dimensionless parameter equal to 0.2948, and $\hbar\omega_p$, the plasmon energy which can often be estimated in the free electron model [27]. Determining the electron density (n) is the key step for calculating the plasmon energy ($\hbar\omega_p$) $n = (N_A \rho Z./M)$ where M is molecular weight, Z represents the quantity of those electrons that contribute to the collective electron oscillations (plasma) while finally, σ represents the relative density or specific gravity.

$$\begin{aligned} \hbar\omega_p &= \hbar\sqrt{ne^2/\varepsilon_0 m} \\ \hbar\omega_p &= \hbar(4\pi ne^2/m)^{1/2} \end{aligned} \qquad (6)$$

where n represents the electronic concentration of the conducting band, e is the elementary charge, m is the electronic mass, ħ is the reduced Planck constant, and ω is the circular plasmon.

The Fermi energy of a metal shifts once it goes through a combination in a chemical reaction and makes a combination to shape a compound. It is known that the X-ray absorbed spectrum of the K or L-edge refers to the displacement of an electron after the corresponding core energy orbital to the original empty position at the Fermi level or just above it [28]. So, if the Fermi level of a metal shifts during a combination in a chemical reaction, its edge of absorption must shift too.

Consequently, the Fermi energy shifts once a compound is made from the metal, and then the variation of energy during this change is:

$$\text{Chemical Shift} = \Delta E_C = E_F^C - E_F^M = \Delta E_F \qquad (7)$$

The assumption $\Delta E_C \approx \Delta E_F$ holds primarily for metallic systems or weakly doped semimetals, where the Fermi level lies near the conduction band. For wide-bandgap semimetals or ionic compounds, additional core-level and ligand-field effects must be considered in interpreting chemical shifts.

Using equation (5), equation (7) becomes:

$$\begin{aligned} \Delta E_C &= A\,[(\hbar\omega_p)_{\text{Compound}}^{4/3} - (\hbar\omega_p)_{\text{Metal}}^{4/3}] \\ \Delta E_C &= 0.2948\,[(\hbar\omega_p)_{\text{Compound}}^{4/3} - (\hbar\omega_p)_{\text{Metal}}^{4/3}] \end{aligned} \qquad (8)$$

Using equations (6-8) we get:

$$\Delta E_F = \Delta E_C = 0.2948\,[((4\pi n_1 e^2/m)^{1/2})_C^{4/3} - ((4\pi n_2 e^2/m)^{1/2})_M^{4/3}] \qquad (9)$$

Where the electronic density (concentration) is represented by n_1 and n_2 within the conduction band of the compound and semimetal, respectively. After simplification, the above equation becomes:

$$\begin{aligned} \Delta E_F &= \Delta E_C = K\,(n_1^{2/3} - n_2^{2/3}) \\ K &= A\hbar^{4/3}\,(e^2/\varepsilon_0 m)^{2/3} \end{aligned} \qquad (10)$$

In the case of chemical shift, ΔE_c = Constant. where Δn is the alteration of the concentration once a metal makes the semimetal, which represents the electronic quantity alteration in the conduction band when any metal forms the compound. It is noteworthy that the present work already mathematically claimed that the plasmon oscillations in Cu are possible during X-ray absorption edge formation.

Equation (10) gives the magnitude of the chemical shift along with the sign, more accurate concerning the electron concentration in the conduction band. It is noteworthy that the quantity of electrons that provides the collective oscillations of electrons (plasma) (Z) of equation (9) is different. The electron concentration is the number of electrons (e) per unit volume (V), which is difficult to calculate for semimetals, but can be assumed to be Z as a first approximation.

2.3. Choice of effective Z

In the present research, the values of Z (electronic quantity participating in collective electron or plasma oscillations) have been carefully selected. Based on the amount of Z, the calculated energy (present research) of plasmon oscillations is comparable to the experimentally detected [28, 29] plasmon loss amount in Zn as well as Cu. The cited articles experimentally observed plasmon-loss values of 10.79 eV and 9.46 eV for Zn and Cu, respectively, which are comparable to the theoretically (references) calculated values of 10.07 eV and 10.79 eV for Zn and Cu, respectively, based on equation (9) (Table 1). Tabular agreement not only justifies the selected Z values for these metals but also confirms that the methodology employed in the present research yields results within experimental error limits. Furthermore, the calculated plasmon-loss values are consistent with the experimentally observed characteristic electron energy-loss values (9.6 eV for Zn and 8.9 eV for Cu), as reported by other authors [30, 31], who also indicate that such losses are expected.

In these models, only delocalized valence electrons, typically those occupying the outer *s* or *p* orbitals, participate actively in collective oscillations, while localized *d* or *f* electrons contribute negligibly due to their restricted mobility. Therefore, the assigned values (*Z = 1* for Cu, *Z = 2* for Zn, *Z = 2* for O, *Z = 3* for N, *Z = 4* for C, *Z = 5* for P, etc.) correspond directly to their electronic configurations and known plasmonic behavior rather than empirical fitting [32]. For example, Cu ($3d^{10}4s^1$) contributes one delocalized 4s electron, while Zn ($3d^{10}4s^2$) contributes two; the values are further supported by experimental plasmon-loss data, which show close correspondence between theoretical and observed plasmon energies.

A sensitivity analysis revealed that a moderate variation of ±10 % in *Z* produces less than a 5 % change in the calculated chemical shift, confirming the model's robustness and demonstrating that its predictive accuracy is not dependent on fine-tuned parameter selection. Hence, *Z* serves as a physically justified and transferable descriptor linking atomic electronic structure with measurable plasmonic and X-ray absorption properties, providing a consistent basis for evaluating chemical shifts across Cu and Zn compounds [24, 33]. The values of Z are adopted from established free-electron and plasmonic models [34,35] and correspond to the number of delocalized valence electrons per atom contributing to plasmon oscillations. They are not fitting parameters but physically derived quantities based on electronic structure and experimental plasmon data.

Table 1. Chemical shift of the various compositions of Cu and Zn.

E/C	**Z**	**ρ**	**M**	**n**	**E_F**	**ΔE_c^1**	**ΔE_c^2**	**(Ref)**
(A) Zn and its various composites								
Zn	**2**	**4**	**65.38**	**10.07**	**6.40**	**--**	**--**	
ZnO	3	5.606	81.38	13.09	9.09	2.69	2.41	**[28]**
$Zn(NO_3)_2$	20	2.065	189.36	13.45	10.64	4.24	3.4 3.96	**[7]** **[28]**
$Zn\ (PO_4)_2$	28	3.75	386.11	15.01	10.91	4.51	4.0	**[7]**
$ZnCO_3$	10	3.5	125.38	15.21	11.10	4.7	4.0 4.25	**[28]** **[7]**
(B) Cu and its various composites								
Cu	**1**	**8.92**	**63.54**	**10.79**	**7.02**	**--**	**--**	
CuI	8	5.62	190.46	13.99	9.93	2.91	2.20	**[29]**
CuO	3	6.40	79.54	14.15	10.08	3.06	3.87 4.4 ± 0.1	**[29]** **[6]**
$CuSO_4$	11	3.60	159.61	15.35	11.24	4.22	4.88 6.6 ± 0.1	**[29]** **[6]**
$Cu(CH_3COO)_2$	31	1.93	181.64	16.52	12.40	5.38	6.7 ± 0.1	**[6]**
$CuCO_3$	11	4.0	123.55	17.18	13.06	6.04	5.6 ± 0.1	**[6]**

E= Element, C=Compound, Z= No of electrons in plasma oscillation participation, ρ = Gravity (Specific), M = Molecular Mass, $\hbar\omega_p$ = Plasmon energy of oscillations, E_F = Fermi Energy, ΔE_c^1= Present Work Chemical Shift, ΔEc^2 = Reference Chemical Shift.

This convention aligns with experimental reports of Cu plasmon energies near 19–21 eV [36-38]. The plasmon energies for Zn (≈16–18 eV) are consistent with this assumption [39,40]. The approximate contributions, O = 2, N = 3, C = 4, H = 1, S = 2, and P = 5, reflect their effective polarizability and role in the overall electronic redistribution within compounds. These assignments are in reasonable agreement with empirical plasmon-loss data and optical constants reported for corresponding materials [36, 38, 41]. It provides a physically meaningful semi-empirical framework linking electron concentration, plasmon energy, and Fermi energy. The approach allows predictive estimation of chemical shifts and plasmonic responses across related systems. Importantly, no arbitrary fitting or parameter adjustment was performed to match specific data points; rather, the adopted Z values are based on widely accepted free-electron models and corroborated by existing experimental evidence. Thus, the parameter Z serves as a realistic descriptor of collective electronic behavior, bridging atomic-level electronic structure with measurable optical and X-ray properties, and ensuring internal consistency between theoretical predictions and observed chemical shifts.

The calculated plasmon and Fermi energies for Zn and Cu compounds reveal systematic variations in chemical shifts that correlate well with reported experimental values. Pure Zn metal exhibits a plasmon energy of 10.07 eV and a Fermi energy of 6.40 eV, which increases upon compound formation due to electron redistribution. ZnO, with a higher density (5.606 g cm^{-3}) and molecular weight (81.38 g mol^{-1}), shows a plasmon energy of 13.09 eV and a Fermi energy of 9.09 eV, resulting in a chemical shift of 2.69 eV, close to the experimental reference value of 2.41 eV [42]. Similar trends are observed for $Zn(NO_3)_2$, $Zn_3(PO_4)_2$, and $ZnCO_3$, with calculated ΔE values of 4.24, 4.51, and 4.70 eV, respectively, which align well with the reported shifts of 3.4–4.0 eV [7,42]. In Cu systems, Cu metal shows a plasmon energy of 10.79 eV and a Fermi energy of 7.02 eV, whereas its compounds display higher plasmon and Fermi energies due to increased conduction electron participation. CuI, CuO, $CuSO_4$, $Cu(CH_3COO)_2$, and $CuCO_3$ exhibit calculated shifts between 2.91 and 6.04 eV, which compare favourably with experimental values ranging from 2.20 to 6.7 eV [6,43]. The methodology combines theoretical modelling with reported experimental data to evaluate chemical shifts in Cu and Zn compounds. The approach correlates Fermi energy with plasmon oscillations, allowing prediction of X-ray absorption edge shifts without direct synchrotron measurements (Figs. 2 and 3).

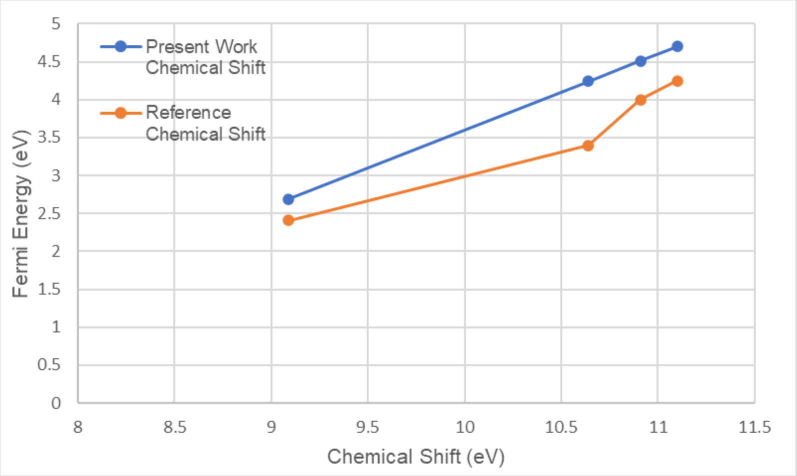

Fig. 2. Variation of chemical shift with Fermi energy for Zn compounds (Complementary to Table 1).

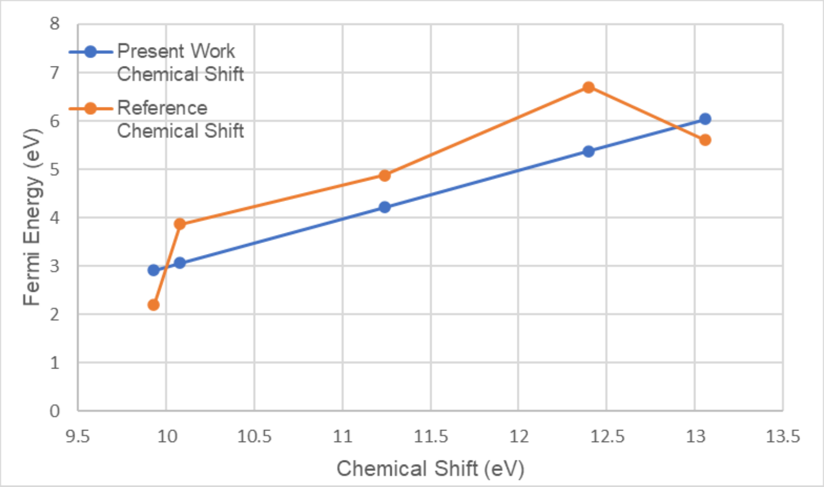

Fig. 3. Variation of chemical Shift with Fermi energy for Cu compounds (Complementary to Table 1).

2.4. *Effective Charge and Fermi Energy*

As reported by the authors [6,44], the absorption edge shift is highly sensitive to the chemical environment surrounding the absorbing atom, which influences factors such as charge distribution, electronegativity, and oxidation state at the atomic interface. The above authors also mentioned that every one of such impacts can be represented in magnitude with ‘‘effective charge’’(q). They further mentioned that the creation of chemical bonds during the compound formation requires a reallocation of the component's electrons associated with the outer or valence electron, along with the effective charge quantity, which is a measurement of the charges that are associated with the cation once it constructs a bond via a ligand.

According to the authors [45], the quantity of the overloaded shift of the Fermi level is associated or correlated properly in conjunction with the effective charge allocation strength. The effective charge relocation energy concept is responsible for the inclination of a shift of the Fermi level [46]. Thus, the point is that the Fermi energy should be a key parameter during chemical shift, along with the effective charge. The values of the effective charge as measured by Joseph et al [6] have been plotted against the present calculated values of Fermi energy for the Cu compounds (Fig. 4), which reveal that there is roughly a linear relation between them, which further supports the present argument that calculation of chemical shift in terms of the Fermi energy could be an alternate method. The effective charge (q), expressed in terms of electrons per atom, provides valuable insights into the electronic environment and bonding characteristics of different metal compounds. For copper-based compounds, the effective charge varies significantly with oxidation state and coordinating groups.

Table 2. Effective charge of some of the Cu and Zn compounds [6,7,44].

Compounds	**Effective charge (q) measured in electrons per atom**
(A) Cu compounds	
CuO	0.75
CuO_3	0.89
$Cu(CH_3COO)_2$	1.01
$CuSO_4$	1.01
(B) Zn compounds	
$Zn(NO_3)_2$	1.55
$Zn_3(PO_4)_2$	1.55
$ZnCO_3$	1.70
$ZnSO_4$	1.70

For instance, CuO exhibits an effective charge of 0.75, while CuO_3 displays a slightly higher value of 0.89, suggesting increased electron withdrawal by oxygen due to stronger oxidation. In organometallic and inorganic salts such as copper acetate ($Cu(CH_3COO)_2$) and copper sulfate ($CuSO_4$), the effective charge reaches 1.01, indicating enhanced ionic character and stronger charge delocalization induced by the acetate and sulfate groups. This higher effective charge is consistent with the increased stability of these complexes in aqueous and biological systems. In comparison, Zn compounds demonstrate a broader range of effective charges, reflecting the highly ionic nature of Zn-ligand interactions. Both zinc nitrate [$Zn(NO_3)_2$] and zinc phosphate [$Zn_3(PO_4)_2$] show an effective charge of 1.55, highlighting the strong electron-withdrawing capacity of nitrate and phosphate anions. Notably, zinc carbonate ($ZnCO_3$) and zinc sulfate ($ZnSO_4$) exhibit even higher values of 1.70, which emphasizes the enhanced ionic polarization and strong electrostatic interactions in these compounds (Table 2). The variation in effective charge among Cu and Zn compounds illustrates how ligand electronegativity, coordination geometry, and oxidation state dictate the overall charge distribution, which in turn influences their solubility, reactivity, and potential applications in catalysis, environmental remediation, and biological systems.

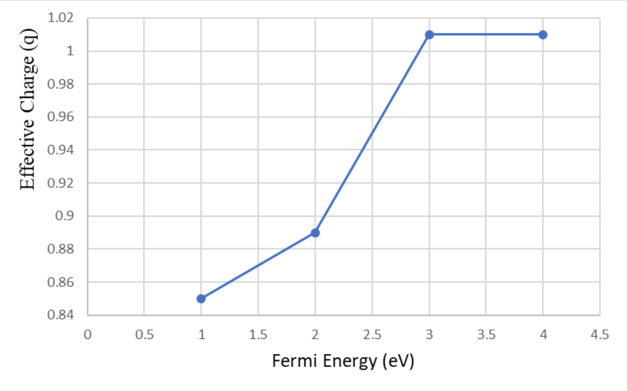

Fig. 4. Variation of Fermi energy with the effective charge of Cu compounds (Complementary to Table 2).

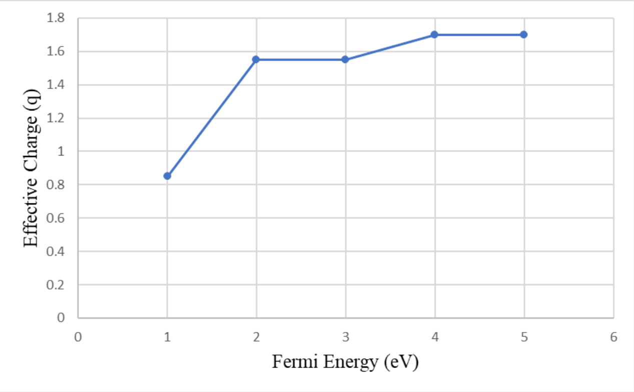

Fig. 5. Variation of Fermi energy with the effective charge of Zn compounds (Complementary to Table 2).

Similarly, for Zn compounds, the effective charge parameter, as reported by the authors [7], has a linear relationship as mentioned in Figure 5.

3. Results and Discussion

Equation (10) clearly explains the nature and thus the positive and negative chemical shifts (depending on whether n_1 is larger or smaller than n_2), while equation (7) explains the amount of chemical shift expressed in the Fermi energy. Using equation (5), one may determine the Fermi energy from the plasmon energy. Plasmon energy of most of the metals is experimentally available, while for the compounds, it can be calculated [30]. Equation (10) further suggests that electronic density (or electronic quantity in one volume) within the conducting energy group changes during chemical shifts, which are responsible for the plasma oscillations. Consequently, the K or L electron occupies the outer band above the Fermi level, which causes a change in the plasmon energy and a disturbance of the electron concentration. When the X-ray falls on a metal surface, the absorption edges shift, creating a metallic bond. The Fermi energy was calculated from the plasmon energy because it was found that the calculated plasmonic energies of Zn and Cu (using Equation (9)) are close to their experimental plasmon values and characteristic values of electron energy. The chemical shift determined in this study is in close agreement with the experimental values reported by different researchers [6,7,43,47]. In some cases, more than one experimentally observed value has been quoted in Table 1.

Derkachova's work on plasma oscillations suggests that plasmon oscillations in dielectrics are physically like those of a metal-sized size [41]. This reality can be further confirmed by the research of Raether [36] and Philipp and Ehrenreich [38], while the work of Gorai and Mahto [48], calculated values show excellent agreement with experimental results of the plasmon energy in semimetals.

Graphs were plotted between the present research and reference values of chemical shifts for Cu and Zn compounds, showing strong agreement, confirming the reliability of the theoretical model. Figures 2 & 3 illustrate a linear relationship between Fermi energy and chemical shift, demonstrating that the Fermi level can serve as a predictive parameter for estimating edge shifts across related compounds. An effective charge, which is an extremely important parameter during the experimental determination of chemical shift, is linearly related to the Fermi energy of Cu and Zn compounds (Figs. 4 & 5), which further supports that the Fermi energy is a central parameter.

The Surface Plasmon Resonance (SPR) discussion has been refined to maintain coherence with the central theme of chemical shift analysis [49]. In this study, the link between SPR and chemical shifts arises through the common dependence of both phenomena on the Fermi energy and conduction electron density of the material. Both the shift in X-ray absorption edges and the excitation of surface plasmons arise from collective electron behavior governed by variations in electron concentration (n) and Fermi level position (E_F). Changes in E_F, calculated from plasmon energy using equation (5), directly affect the energy of plasmonic oscillations, thereby linking the chemical shift mechanism to plasmonic responses. Consequently, SPR is discussed here not as an isolated phenomenon but as an extended manifestation of the same electronic redistribution that influences X-ray absorption edge shifts in Cu and Zn systems [50]. This conceptual link highlights the broader significance of Fermi energy in explaining both spectroscopic and optical behaviors of metallic and semiconducting compounds, while no new experimental SPR data are claimed in the present work. In this context, the calculated Fermi energies and plasmon energies for Cu and Zn compounds provide a theoretical foundation for understanding their SPR characteristics. Theoretical consistency check that aligns with the established optical and electronic behavior of Cu and Zn. The observed correlation between Fermi-level variation and plasmon energy suggests that the same electronic parameters influencing chemical shifts in X-ray absorption also modulate plasmon resonance frequencies in the optical domain. The discussion illustrates a conceptual extension of the Fermi-energy framework, showing that the derived electronic parameters are consistent with the known plasmonic behaviors of Cu and Zn reported in the literature. The revised interpretation thus maintains internal consistency between the X-ray absorption analysis and the plasmonic phenomena. Cu-based materials show exceptional compassion for plasmonic biosensors. Stebunov et al. said that plasmonic biosensors are responsible for SPR technology and are inexpensive, offering a foundation for efficient biosensors incorporated into contemporary electronic devices [51]. Stern and Farrell considered the technique of resonance settings, for the first time, projected the notion of surface plasmon [52], namely, a plasmonic behavior of unrestricted electronic field adjacent to a conducting band close to Fermi energy around the metal or externally controlled via electric and magnetic energy [53]. Consequently, the Fermi level is a crucial model for the SPR. It is noteworthy that the nature of the Fermi level in Cu and Zn, and their chemical composition, make it difficult for them to shift their Fermi levels.

The biggest of the investigational conclusions on surface plasmons are confined to noble metals. However, the authors suggested that Cu can arise as a hopeful SPR nominee [54-58]. These authors [54] noted that quantum dots of Cu oxide can be effectively manufactured utilizing the technique of chemical reduction or drop technique due to the nature of its Fermi energy, conduction bandwidth, and surface sensitivity. The mass reduction led to astonishing alterations in their optical retorts as contrasted to the bulk metal. This retort varies as the volume, form, and insulating nature of the particles of nano-size. They went on to say that [54] quantum limitation led to a change in the metal's insulator constant at very small particle sizes. It causes SPR to grow when its volume decreases. It is noteworthy that the transition energy required for the inter-band transition in Cu is lower than the transition energies [59]. This implies a hurdle to the transition within the zone, which leads to a significant damping constant. Coupled with the metallic mass of copper, the SPR frequency progressively shifts towards an extended wavelength when the volume of the metal decreases owing to the impact of the surface. Thus, according to these authors [59], the issues for which plasmon resonance frequency is affected should be the medium and the insulator (or dielectric) constant of stuff including the geometrically linked magnitude of shapes of particles of nano-size and hence the Fermi energy and the conduction bandwidth.

As reported by the above author [59], the dielectric constant of the medium, form, as well as of volume, where the sole metal particles of nano size Cu characterize, govern the rate of recurrence of SPR, and its time period is nearly about 10 fs under 2.2 eV incoming photons (energy) interact with nanogold spheres. The authors also [59] found that it is feasible to have larger photo-production (over 2.0 eV) when the energy of the heated electronic beam is contrasted by the Fermi energy intensity, though the warmed hole's energy (lesser E_F) was projected to be about 1.0 eV. Moreover, the Fermi energy of Cu, as mentioned, is 7.01 eV [60], which is awfully close as calculated in the present research as 7.02 eV (Table 1). Thus, we see that Cu metal can offer an important option for the expansion of effective, minimal-cost, and small-loss plasmonic nanoparticles, and choosy nano-catalysts. Thus, it is beyond doubt that copper, being inexpensive and extra plentiful in the environment, is being utilized in a massive quantity as an energy mover because of its properties, mainly, Fermi energy, dielectric constant, and bandwidth. Several studies have suggested that Cu and Zn are promising candidates for SPR-based applications due to their characteristic Fermi energies, conduction bandwidths, and dielectric properties [61]. Cu, in particular, exhibits tunable plasmon resonance peaks between 600 and 1100 nm, making it suitable for low-cost plasmonic biosensors and photocatalysts [62, 63]. The Cu nanoparticles (NPs) detected peak frequency in between visible range to near-infrared red with tunable plasmonic frequency. Cu NPs are low-cost synthetic resources with promising activity that reflects the significant character of the particles. One of the primary challenges in the synthesis of Cu NPs is its susceptibility to oxidation, which is exacerbated at the nanometric size and necessitates. According to some authors [64] the curve of dispersion of SPR of Cu indicated that there is an occurrence of resonance at a sharp absorption edge at 2.16 eV due to the transition difference between the d-band to Fermi energy level, such change triggers a significant role around the position of plasmon at outside (surface) and produces the genuine resonance to happen in the complicated frequency region.

On the other hand, a model on Zn NPs surface plasmon resonance has been suggested by some workers [65], where it can be noticed that it also has some of the above properties. However, according to these workers [65], excitation of PR (plasmon resonance) for the nano particle size of Zn is possible within the range of 200 nm to 400 nm. Several researchers have conducted research investigations on resonance involving plasmons with Zn particles of the nanoscale attained by diverse techniques [66-69]. The majority of these workers mentioned that plasmon resonance is possible within the liquid or inside a Silicon Oxide (SiO_2). Zn is also susceptible to plasmonic surface oscillations, and this is the easiest issue related to the nanosphere for the void or vacuum. Due to its suitable dielectric constant, which is susceptible to plasmon vibrations, its Fermi energy nature, and the spherical shape of the normal Zn nanoparticle, it is more susceptible to plasmonic surface vibrations and therefore to SPR. For a few semimetals, the discrepancy between an experiment and theoretical chemical shifts, numerical magnitude could be possible since we used an estimated but simple technique to determine the Fermi energies, and the formula of equation (5) applies at absolute zero temperature, where only the ground state oscillators participate in the plasmon. There is an influence of temperature, shielding, etc.

4. Conclusion

This study presents a refined theoretical model linking Fermi energy, plasmon energy, and effective charge to predict chemical shifts in Cu and Zn compounds with strong consistency to experimental results. The method eliminates the need for empirical parameters and provides a unified explanation of both X-ray absorption edge shifts and plasmonic behavior. Correlating Fermi-level variations with plasmonic behavior, thereby offering a unified explanation for electronic redistribution during compound formation. Moreover, the approach extends the concept of Fermi energy beyond X-ray absorption analysis to include its influence on surface plasmon resonance (SPR), providing an integrated understanding of optical and spectroscopic properties. The SPR discussion complements it rather than distracts it from the main findings on Fermi energy and chemical shifts. This dual relevance makes the model applicable not only to Cu and Zn but also to other transition metals and semiconducting systems. SPR is prominent in Cu and Zn compounds under certain circumstances, and due to the nature of the Fermi energy, conduction bandwidth, and dielectric constant, its applications in SPR-related nano-devices are inevitable. The work contributes both conceptual and methodological novelty by simplifying the complex relationship between electronic structure and experimentally observed edge shifts.

Acknowledgements

The present author is grateful to the G.B. Pant University, U. P State of Higher Education Council and Uttaranchal University for their constant encouragement throughout this work.

Funding Statement

This research received no specific grant from any funding agency.

Conflicts of interest

The authors declare that they have no known competing financial interests or personal relationships that could have appeared to influence the work reported in this paper.

Authors contribution statement

Ajay Kumar (Corresponding Author) conceived the research idea, designed the methodology, analyzed the data, reviewed and provided critical suggestions for improvement. Tikaram contributed to data collection, literature review, and assisted in theoretical derivations. Dinesh Kumar supported in result interpretation and validation. Poonam Juneja and Sanjeev Rathore contributed to data curation, figure preparation, and technical editing. Hari Krishan developed the theoretical framework, and prepared the original draft of the manuscript Narinder Kumar analyzed the data, literature review, and assisted in theoretical derivations. All data included in this paper are available upon request by contacting the corresponding author.

References

[1] Agarwal, B.K. and Verma, L.P., 1970. A rule for chemical shifts of X-ray absorption edges. *Journal of Physics C: Solid State Physics*, 3(3), p.535.

[2] Pan, J., Gao, B., Guo, K., Gao, Y., Xu, X. and Yue, Q., 2022. Insights into selective adsorption mechanism of copper and zinc ions onto biogas residue-based adsorbent: Theoretical calculation and electronegativity difference. *Science of the Total Environment*, *805*, p.150413.

[3] Singh, V.P., Singh, S., Singh, D.P., Singh, P., Tiwari, K., Mishra, M. and Butcher, R.J., 2013. Synthesis, spectral and single crystal X-ray diffraction studies on Co (II), Ni (II), Cu (II) and Zn (II) complexes with o-amino acetophenone benzoyl hydrazone. *Polyhedron*, *56*, pp.71-81.

[4] Kawata, S. and Maeda, K., 1973. Effects of chemical combination on the X-ray LIII absorption limits of Mo, Rh, Pd, Ag and Cd. *Journal of Physics F: Metal Physics*, 3(1), p.167.

[5] Salem, S.I., Chang, C.N., Lee, P.L. and Severson, V., 1978. Energy shift of the K-absorption edge of Mn and Fe compounds. *Journal of Physics C: Solid State Physics*, 11(19), p.4085.

[6] Joseph, D., Basu, S., Jha, S.N. and Bhattacharyya, D., 2012. Chemical shifts of K X-ray absorption edges on copper in different compounds by X-ray absorption spectroscopy (XAS) with synchrotron radiation. *Nuclear Instruments and Methods in Physics Research Section B: Beam Interactions with Materials and Atoms*, 274, pp.126–128.

[7] Joseph, D. and Patra, N., 2017. Chemical shift at the X-ray K-absorption edge of Zn in some Zn compounds. *Madridge Journal of Analytical Sciences and Instrumentation*, 2(1), pp.25–27.

[8] Rudolph, J. and Jacob, C.R., 2018. Revisiting the dependence of Cu K-edge X-ray absorption spectra on oxidation state and coordination environment. *Inorganic Chemistry*, 57(17), pp.10591–10607.

[9] Batail, P., 2004. Introduction: molecular metals. *Chemical Reviews*, 104(11), pp.4887–4890.

[10] Pendharkar, A.V. and Mande, C., 1973. Fine structure of the rhenium LIII absorption discontinuity. *Physica*, 66(1), pp.204–210.

[11] Tzeng, C.T., Lo, W.S., Yuh, J.Y., Chu, R.Y. and Tsuei, K.D., 2000. Photoemission, near-edge X-ray absorption spectroscopy, and low-energy electron-diffraction study of C_{60} on Au (111) surfaces. *Physical Review B*, 61(3), p.2263.

[12] Solomon, E.I., Hedman, B., Hodgson, K.O., Dey, A. and Szilagyi, R.K., 2005. Ligand K-edge X-ray absorption spectroscopy: covalency of ligand–metal bonds. *Coordination Chemistry Reviews*, 249(1–2), pp.97–129.

[13] Ma, Q., Prater, J.T., Sudakar, C., Rosenberg, R.A. and Narayan, J., 2012. Defects in room-temperature ferromagnetic Cu-doped ZnO films probed by X-ray absorption spectroscopy. *Journal of Physics: Condensed Matter*, 24(30), 306002.

[14] Zhao, W., Wen, L., Parkin, I.P., Zhao, X. and Liu, B., 2023. Fermi-level shift, electron separation, and plasmon resonance change in Ag nanoparticle-decorated TiO_2 under UV light illumination. *Physical Chemistry Chemical Physics*, 25(29), pp.20134–20144.

[15] Dekker, A.J., 2017. *Solid State Physics.* Macmillan Indian Ltd.

[16] Pines, D., 2018. *Elementary Excitations in Solids.* CRC Press.

[17] Elzinga, E.J. and Reeder, R.J., 2002. X-ray absorption spectroscopy study of Cu^{2+} and Zn^{2+} adsorption complexes at the calcite surface: Implications for site-specific metal incorporation preferences during calcite crystal growth. *Geochimica et Cosmochimica Acta*, *66*(22), pp.3943-3954.

[18] Minamimoto, H., Yasuda, K., Zhou, R., Li, X., Yasuda, S. and Murakoshi, K., 2020. Potential energy shift of the Fermi level at plasmonic structures for light-energy conversion determined by graphene-based Raman measurements. *The Journal of Chemical Physics*, *152*(12).

[19] Saxena, N.N., Gupta, S.N. and Anihindi, R.G., 1974. Chemical shift of zinc K-absorption edge in some compounds. *Journal of Physics and Chemistry of Solids*, 35(10), pp.1451–1452.

[20] Zhao, X.Z., Jiang, T., Wang, L., Yang, H., Zhang, S. and Zhou, P., 2010. Interaction of curcumin with Zn (II) and Cu (II) ions based on experiment and theoretical calculation. *Journal of Molecular Structure*, *984*(1-3), pp.316-325.

[21] Verma, L.P. and Agarwal, B.K., 1968. Shifts in the X-ray K-absorption edge of copper due to chemical effects. *Journal of Physics C: Solid State Physics*, 1(6), p.1658.

[22] Li, Y. and Korzhavyi, P.A., 2017. Physical and chemical properties of Cu (I) compounds with O and/or H. *Dalton Transactions*, *46*(2), pp.529-538.

[23] Rößler, N. and Staemmler, V., 2003. Ab initio calculations for the 2s and 2p core level binding energies of atomic Zn, Zn metal, and Zn-containing molecules. *Physical Chemistry Chemical Physics*, *5*(17), pp.3580-3586.

[24] Morton, S.M., Silverstein, D.W. and Jensen, L., 2011. Theoretical studies of plasmonics using electronic structure methods. *Chemical reviews*, *111*(6), pp.3962-3994.

[25] Halas, N.J., Lal, S., Chang, W.S., Link, S. and Nordlander, P., 2011. Plasmons in strongly coupled metallic nanostructures. *Chemical reviews*, *111*(6), pp.3913-3961.

[26] Srivastava, K.S., Singh, S., Gupta, P., Srivastava, A.K., Kumar, V., Husain, M. and Prasad, M.K., 1981. X-ray K-absorption edge shifts due to chemical combination. *Pramana*, *17*(2), pp.187-192.

[27] Akbari-Moghanjoughi, M., 2023. Energy Band Structure of Relativistic Quantum Plasmon Excitation. *arXiv preprint arXiv:2303.04881*.

[27] Baker, M.L., Mara, M.W., Yan, J.J., Hodgson, K.O., Hedman, B. and Solomon, E.I., 2017. K- and L-edge X-ray absorption spectroscopy (XAS) and resonant inelastic X-ray scattering (RIXS) determination of differential orbital covalency (DOC) of transition metal sites. *Coordination Chemistry Reviews*, 345, pp.182–208.

[28] Saxena, N.N., Gupta, S.N. and Anihindi, R.G., 1974. Chemical shift of zinc K-absorption edge in some compounds. *Journal of Physics and Chemistry of Solids*, 35(10), pp.1451–1452.

[29] Verma, L.P. and Agarwal, B.K., 1968. Shifts in the X-ray K-absorption edge of copper due to chemical effects. *Journal of Physics C: Solid State Physics*, 1(6), p.1658.

[30] Paterson, P.J.K. and Leckey, R.C.G., 1974. Characteristic energy losses in zinc and cadmium. *Journal of Physics F: Metal Physics*, 4(6), L156.

[31] Velu, S., Suzuki, K., Vijayaraj, M., Barman, S. and Gopinath, C.S., 2005. *In situ* XPS investigations of $Cu_{1-x}Ni_xZnAl$ mixed metal oxide catalysts used in the oxidative steam reforming of bio-ethanol. *Applied Catalysis B: Environmental*, 55(4), pp.287–299.

[32] Krishchenko, I.M., Manoilov, É.G., Kravchenko, S.A. and Snopok, B.A., 2020. Resonant optical phenomena in heterogeneous plasmon nanostructures of noble metals: a review. *Theoretical and Experimental Chemistry*, *56*(2), pp.67-110.

[33] Huang, H.B., Yu, K., Zhang, N., Xu, J.Y., Yu, X.T., Liu, H.X., Cao, H.L., Lü, J. and Cao, R., 2020. Localized surface plasmon resonance enhanced visible-light-driven CO_2 photoreduction in Cu nanoparticle loaded ZnInS solid solutions. *Nanoscale*, *12*(28), pp.15169-15174.

[34] Jian, C.C., Zhang, J. and Ma, X., 2020. Cu–Ag alloy for engineering properties and applications based on the LSPR of metal nanoparticles. *RSC advances*, *10*(22), pp.13277-13285.

[35] Leon, D.A., Cardoso, C. and Berland, K., 2025. Bulk plasmons in elemental metals. *arXiv preprint arXiv:2510.07261*.

[36] Raether, H. (2006). *Excitation of plasmons and interband transitions by electrons.* Springer, Berlin, pp. 23–34.

[37] Vehse, R.C. and Arakawa, E.T., 1969. Optical and photoemissive properties of nickel in the vacuum-ultraviolet spectral region. *Physical Review*, 180(3), 695–705.

[38] Philipp, H.R. and Ehrenreich, H., 1963. Optical properties of semimetals. *Physical Review*, 129(4), 1550–1560.

[39] Tomaev, V.V., Polishchuk, V.A., Vartanyan, T.A. and Vasil'ev, E.A., 2019. Surface plasmon resonance in zinc nanoparticles. *Glass Physics and Chemistry*, 45, 238–241.

[40] Amekura, H., Shinotsuka, H. and Yoshikawa, H., 2017. Are the triple surface plasmon resonances in Zn nanoparticles true? *Nanotechnology*, 28(49), 495712.

[41] Derkachova, A., Kolwas, K. and Demchenko, I., 2016. Dielectric function for gold in plasmonics applications: size dependence of plasmon resonance frequencies and damping rates for nanospheres. *Plasmonics*, 11, pp.941–951.

[42] Saxena, N.N., Gupta, S.N. and Anihindi, R.G., 1974. Chemical shift of zinc K-absorption edge in some compounds. *Journal of Physics and Chemistry of Solids*, 35(10), pp.1451–1452.

[43] Verma, L.P. and Agarwal, B.K., 1968. Shifts in the X-ray K-absorption edge of copper due to chemical effects. *Journal of Physics C: Solid State Physics*, 1(6), p.1658.

[44] Chaboy, J., Muñoz-Páez, A., Carrera, F., Merkling, P. and Marcos, E.S., 2005. *Ab initio* X-ray absorption study of copper K-edge XANES spectra in Cu(II) compounds. *Physical Review B*, 71(13), 134208.

[45] Levlev, V.M. and Shvedov, E.V., 2018. *Physics of the Solid State*, 44(3), 144–149.

[46] Matsumoto, Y., Katayama, M., Abe, T., Ohsawa, T., Ohkubo, I., Kumigashira, H. and Koinuma, H., 2010. Chemical trend of Fermi-level shift in transition metal-doped TiO_2 films. *Journal of the Ceramic Society of Japan*, 118(1383), pp.993–996

[47] Lourenço, M.A., Zeng, J., Jagdale, P., Castellino, M., Sacco, A., Farkhondehfal, M.A. and Pirri, C.F., 2021. Biochar/zinc oxide composites as effective catalysts for electrochemical CO_2 reduction. *ACS Sustainable Chemistry & Engineering*, 9(15), pp.5445–5453.

[48] Gorai, S.K. and Mahto, P., 2013. Correlation between ground state properties and plasmon energy of ternary chalcopyrite semimetals. *IOSR Journal of Applied Physics*, 3, pp.19–23.

[49] Link, S. and El-Sayed, M.A., 1999. Size and temperature dependence of the plasmon absorption of colloidal gold nanoparticles. *The Journal of Physical Chemistry B*, 103(21), 4212–4217.

[50] Brouder, C., Alouani, M. and Arnaud, B., 2004. Electronic structure and X-ray absorption edges of Cu and Zn compounds: Relation to plasmonic and charge-transfer effects. *Physical Review B*, 70, 045119.

[51] Stebunov, Y.V., Yakubovsky, D.I., Fedyanin, D.Y., Arsenin, A.V. and Volkov, V.S., 2018. Superior sensitivity of copper-based plasmonic biosensors. *Langmuir*, 34(15), pp.4681–4687.

[52] Stern, E.A. and Ferrell, R.A., 1960. Surface plasma oscillations of a degenerate electron gas. *Physical Review*, 120(1), pp.130.

[53] Lal, S., Link, S. and Halas, N.J., 2007. Nano-optics from sensing to waveguiding. *Nature Photonics*, 1(11), pp.641–648.

[54] Geetha, P.P., Ramachandran, A. and Nair, S.S., 2020. Tuning of localized surface plasmon resonance in copper–copper oxide core–shell quantum dots for biosensor applications.

[55] Cortez-Valadez, M., Bocarando-Chacon, J.G., Hernández-Martínez, A.R., Hurtado, R.B., Alvarez, R.A., Roman-Zamorano, J.F. and Flores-Acosta, M., 2014. Optical properties and radial breathing modes present in Cu amorphous quantum dots obtained by green synthesis. *Nanoscience and Nanotechnology Letters*, 6(7), pp.580–583.

[56] Indhu, A.R., Dharanya, C. and Dharmalingam, G., 2024. Plasmonic copper: ways and means of achieving, directing, and utilizing surface plasmons. *Plasmonics*, *19*(3), pp.1303-1357.

[57] Pillai, A.M., Nair, N., Das, M.K. and Ram, S.K., 2025. Strategic approaches to enhance efficiency and commercial feasibility of copper-based surface plasmon resonance sensing. *Next Materials*, *7*, p.100377.

[58] Park, B.K., Jeong, S., Kim, D., Moon, J., Lim, S. and Kim, J.S., 2007. Synthesis and size control of monodisperse copper nanoparticles by polyol method. *Journal of Colloid and Interface Science*, 311(2), pp.417–424.

[59] Devasenathipathy, R., Wu, D.Y. and Tian, Z.Q., 2019. Surface plasmon enhanced chemical reactions on metal nanostructures. In: *Nanoplasmonics.* IntechOpen

[60] Martínez-Ruiz, A., Moreno, M.G. and Takeuchi, N., 2003. First-principles calculations of the electronic properties of bulk Cu_2O, clean and doped with Ag, Ni, and Zn. *Solid State Sciences*, 5(2), pp.291–295.

[61] Liu, J., Jalali, M., Mahshid, S. and Wachsmann-Hogiu, S., 2020. Are plasmonic optical biosensors ready for use in point-of-need applications?. *Analyst*, *145*(2), pp.364-384.

[62] Reddy, K.R., Hassan, M. and Gomes, V.G., 2015. Hybrid nanostructures based on titanium dioxide for enhanced photocatalysis. *Applied Catalysis A: General*, 489, 1–16.

[63] Hutter, E. and Fendler, J.H., 2004. Exploitation of localized surface plasmon resonance. *Advanced Materials*, 16(19), 1685–1706.

[64] Jiang, Q., Ji, C., Riley, D.J. and Xie, F., 2018. Boosting the efficiency of photoelectrolysis by the addition of non-noble plasmonic metals: Al and Cu. *Nanomaterials*, 9(1), p.1.

[65] Tomaev, V.V., Polishchuk, V.A., Vartanyan, T.A. and Vasil'ev, E.A., 2019. Surface plasmon resonance in zinc nanoparticles. *Glass Physics and Chemistry*, 45, pp.238–241.

[66] Ievlev, V.M. and Shvedov, E.V., 2006. Kinetics of formation of discrete nanostructures during vacuum condensation from a single-component vapor. *Physics of the Solid State*, *48*(1), pp.144-149.

[67] Amekura, H., Shinotsuka, H. and Yoshikawa, H., 2017. Are the triple surface plasmon resonances in Zn nanoparticles true? *Nanotechnology*, 28(49), 495712.

[68] Rajamanickam, U., Mylsamy, P., Viswanathan, S. and Muthusamy, P., 2012. Biosynthesis of zinc nanoparticles using actinomycetes for antibacterial food packaging. In: *International Conference on Nutrition and Food Sciences IPCBEE*, Vol. 39.

[69] Singh, S.C. and Gopal, R., 2007. Zinc nanoparticles in solution by laser ablation technique. *Bulletin of Materials Science*, 30, pp.291–293.